Polymer 50 (2009) 317–327

Contents lists available at ScienceDirect

Polymer

journal homepage: www.elsevier.com/locate/polymer

A quantum mechanical study on polymer flexibility: Extended model from monomer to tetramer of 2- and 4-bromostyrenes

Amparo Navarro [a,*], M. Paz Fernández-Liencres [a], Tomás Peña-Ruiz [a], José Manuel Granadino-Roldán [a], Manuel Fernández-Gómez [a], Gustavo Domínguez-Espinosa [b], María J. Sanchís [b]

[a] Department of Physical and Analytical Chemistry, University of Jaén, Campus Las Lagunillas, 23071 Jaén, Spain
[b] Department of Applied Thermodynamics, ETSII Polytechnic University of Valencia, Camino de Vera s/n 46071 Valencia, Spain

ARTICLE INFO

Article history:
Received 29 August 2008
Accepted 16 October 2008
Available online 5 November 2008

Keywords:
Bromostyrenes
DFT calculations
Glass transition temperature

ABSTRACT

DFT Quantum chemical descriptors as dipole and quadrupole momenta as well as molecular volume have been calculated for the monomer, dimer and tetramer of 2- and 4-bromostyrene in order to study the effect of small changes in their molecular structure on the glass transition temperature of the corresponding polymers. In addition, correlation with the chain stiffness has been pursued by analysing torsional barriers both for monomer and oligomers of the title compounds obtained at *ab initio* and DFT levels of theory. First of all, the performance of the theoretical methods has been checked by optimizing the molecular geometry of the monomer and comparing with experimental data. The internal rotation barrier of the vinyl moiety has been also calculated and a conformational analysis has been afforded in detail through different energy factorization schemes, i.e., the total kinetic and potential scheme and that provided by the NBO theory. In addition, the topological analysis of the electron density provided by the Atom-in-Molecules, AIM, theory has allowed us to rationalize the stable conformers on the basis of bond critical points and ring critical points featuring intramolecular contacts. The most stable conformations of the dimer and tetramer have been determined as models for their respective polymers. The values of the central dihedral angles for the most populated dimer and tetramer of both 2- bromo and 4-bromostyrene indicate that the position of the halogen hardly affects the backbone chain arrangement. Predictive performance of the internal rotation barriers as well as the molecular volume and dipole and quadrupole momenta have been assessed through comparison with the experimental T_g value for the title compounds. As a conclusion, although the internal rotation barrier does not provide conclusive results for the higher chain flexibility in the case of poly-2-bromostyrene, the dipole and quadrupole momenta, as well as the molecular volume calculated for the monomer, dimer and tetramer follow the same trend as the measured T_g for poly-2-bromostyrene and poly-4-bromostyrene demonstrating this way the capability of those descriptors for predicting small variations in glass transition temperatures.

1. Introduction

A lot of effort has been devoted so far to predict and explain different polymer properties from a molecular point of view. One of the most important ones in amorphous polymers, the glass transition temperature, T_g, is influenced by several chemical structure-dependent features as the stiffness of the chain, the free volume and interactions between neighboring chains. The chain flexibility is controlled by the rotation of the C–C backbone. Low internal rotation barriers should result in a more flexible polymer, and therefore, a lower glass transition temperature, T_g. The free volume takes account of the space needed for the chains for coordinated molecular motion leading to reptation. In the case of interactions between chains, the corresponding intermolecular potential will depend, among others, on the relative values of the multipole moments [1–3].

In the last years several works have emerged dealing with the prediction of T_g from different quantum mechanical descriptors determined by means of QSPR approaches. Thus, Yu et al. [4,5] performed a correlation between the T_g and the molecular volume, the quadrupole and hexadecapole moments. Liu et al. [6] also performed a QSPR study on the glass transition temperature of polyacrylates using LUMO and HOMO energies, positive charges and dipole moments as descriptors. Furthermore, the prediction of thermal decomposition property of polymers was studied by Yu et al. [7] using as quantum chemical descriptors the quadrupole moment and the total energy.

In this paper we focus our attention on the pendant-group polymers, which are very interesting from a theoretical point of

* Corresponding author.
E-mail address: anavarro@ujaen.es (A. Navarro).

0032-3861/$ – see front matter © 2008 Published by Elsevier Ltd.
doi:10.1016/j.polymer.2008.10.041

view since the pi-electrons reside on these pendant groups and there is generally no conjugation path along the chain backbone. Polystyrene constitutes a prototype for this class of pendant-group polymers. These materials consist of a saturated backbone on which aromatic side groups (phenyl groups) are attached. The saturated backbone allows rotation around C–C single bonds while the aromatic rings are suitable to establish pi–pi interactions among neighboring rings. The nature of those interactions has been subject of interest from many years due to their role determining the intermolecular potential, and as consequence, the preferred modes of packing of the aromatic rings in amorphous polymers such as polystyrene, structure in proteins and DNA, etc. (see Ref. [8] and references therein). As an approximation to the intermolecular contacts, the benzene dimer interaction has also been studied by different authors as prototype of pi–pi interactions showing that the contribution of the electrostatic quadrupole–quadrupole interaction is significant as compared to the remaining dispersion and exchange–repulsion contributions [9–13]. For styrene, the majority of the published work is concerned with the structure of the monomer [14,15] but there has been little analysis of the fundamental interactions in the styrene dimer and polymer [16–19]. An earlier electron diffraction study on thin films of polymers of *p*-chloro-, *p*-bromo-, and *p*-iodostyrene concluded that the benzene rings are located alternately on each side of the plane of the zig-zag paraffin chain and the neighboring molecules are closely packed in a "face-to-face" configuration in a plane perpendicular to the chain [20].

The halogenated forms of polystyrene are commercialized in order to turn that material into a flame retardant polymer [21,22]. The most common halo-substitutions are *ortho* and *para* chloro and bromo substitutions. Bromostyrene polymers are useful as flame retardants for thermoplastics bestowing improved fire resistance as well as color retention after molding. The syntheses by radical polymerization of *ortho*-, *meta*-, and *para*-monobrominated styrenes were described in the literature by Horie et al. [23], who also determined that the glass transition temperature increases from I to II [23,24].

In 2001, Thaweephan et al. [25] studied the effect of the aromatic substitution on halogenated polystyrenes and their blends on T_g and found that of poly-4-bromostyrene is higher than that of polystyrene as well as those of *ortho* or *meta* bromoderivatives. In order to explain that behaviour, they performed an energy barrier calculation using the MM+ molecular mechanics force field for eight styrene segments. The torsion potentials were calculated rotating in turn half of the chain around the central link. They obtained a rotation barrier for 4-bromostyrene smaller than those of the *meta* and *ortho* substitutions while T_g show the opposite trend. They proposed a plausible but not conclusive explanation by which the Br atoms which are protruding out from the styrene side group could establish interchain molecular interactions which could hinder the motion giving rise to an increase in T_g.

The goal of the present work is to get more insight from a theoretical point of view into the variation of the properties on which depends the T_g in poly-bromostyrenes when small changes are produced in the molecular structure of the repetitive unit. This could be the case of the *ortho* and *para* bromine substitution in polystyrene for which the shift in T_g is less than 10 °C. To achieve this, we will analyze three molecular properties determined by Density Functional Theory, all of which have been previously selected in QSPR studies yielding satisfactory results for the prediction of T_g [4–7]. Those properties will be calculated not only for the monomer but also for the dimer and tetramer in order to analyze their variation with the size of the molecular system. We have chosen the dipole and quadrupole moments as factors influencing the intermolecular potential, and the molecular volume as a first approximation to the space which is needed by the molecule for reptation. We are interested in determining how sensitive are those quantum mechanical descriptors to small variations in T_g.

This work is organized as follows: molecular structure and internal rotation barriers for the monomers of 2- bromostyrene and 4-bromostyrene are investigated in order to check the performance of the different theoretical methods essayed. After that, the stable conformations of the dimer and tetramer will be determined as models for their respective polymers, trying to obtain a correlation between the aforementioned molecular properties when the bromine atom goes from the *ortho* to the *para* position and the glass transition temperature. In addition, the internal rotation barrier around the central dihedral angle in the tetramer is determined in order to extract some conclusion about the relative stiffness of the chains. As the measured T_g shows different values depending on the experimental conditions, we have obtained our own values using the same experimental procedure for both poly-bromoderivatives.

2. Computational details

The Gaussian03 [26] suite of programs was used to carry out the *ab initio* and DFT calculations running on an ia64HP server rx 2600. Calculations were performed using standard gradient techniques at the MP2 [27] and DFT levels. On the one hand, Pople's 6-31G* and 6-311++G** [28] basis sets were used as examples of small and large basis developed for molecular orbital (MO) calculations. Furthermore, Dunning's correlation consistent basis set of medium size, cc-PVDZ [29], was also essayed. As exchange functional, Becke's hybrid exchange was used, B3 [30], and as correlation functional the Lee–Yang–Parr non-local functional, LYP [31,32]. Also, the mPW1PW91 model was used as a modified Perdew–Wang exchange functional and Perdew–Wang 91 correlation [33] in order to assess the effect of the different HF exchange percentage (20% and 25%, respectively) either on the molecular structure and the torsional barrier.

B3LYP, mPW1PW91 and MP2 were essayed in combination with the small 6-31G* basis set in order to check the effect of the method in the molecular of the monomer and comparing with experimental data. Furthermore, taking into account that B3LYP functional is one of the most standard method in the field of polymers, the three afore described basis set, 6-31G*, cc-PVDZ and 6-311++G** were essayed in order to check the effect of the size of the basis set.

The nature of the stationary points was assessed through the vibrational wavenumbers calculated from analytical second derivatives concluding that all of them were real minima.

The rotational barrier of the vinyl–phenyl torsion at B3LYP level was calculated using the 6-31G*, 6-311++G** and cc-PVTZ basis sets. For mPW1PW91 and MP2 methods only the 6-31G* was essayed. All calculations were performed in a relaxed way, that is, fixing only the dihedral C4–C3–C1–C8 and relaxing all the other parameters. Total energy surfaces have been constructed in steps of 10° using default convergence criteria as implemented in Gaussian03.

Molecular volumes of the previously optimized structures were calculated as the volume inside a contour of 0.001 electrons/bohr^3 density envelope [34]. A Monte–Carlo integration method with increased accuracy requested via "volume = tight" keyword within Gaussian03 was essayed.

The quadrupole moment tensor [35] was calculated by Gaussian03 and the tensor itself is diagonalized, transforming it into its traceless form with $\theta_{zz} = -\theta_{xx} - \theta_{yy}$. According to Eubank's equation [36], an effective quadrupole moment can be then obtained according to:

$$\theta_{\text{eff}} = \left[\frac{2}{3}(\theta_{xx}^2 + \theta_{yy}^2 + \theta_{zz}^2)\right]^{1/2}$$

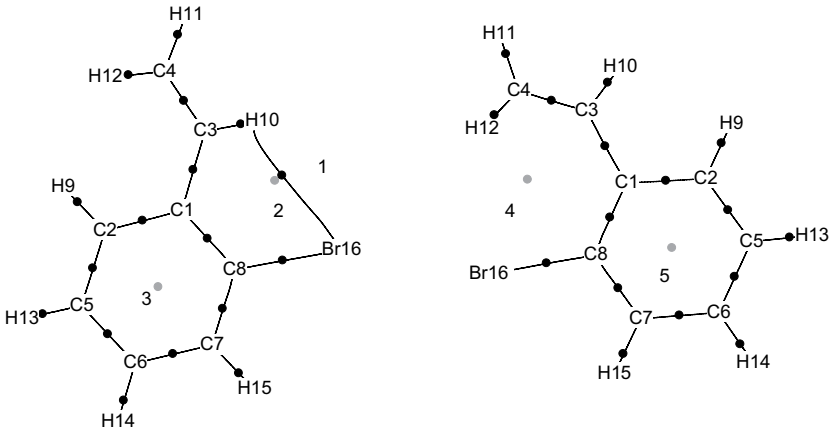

Fig. 1. Molecular structure of the *trans* (left) and *cis* (right) conformers of 2-bromostyrene showing atom numbering. For the 4-bromostyrene the numbering atom is the same changing the bromine atom from the position number 16 to the position number 14.

where θ_{xx}, θ_{yy} and θ_{zz} are the values of the quadrupole moment tensor in the *x*-, *y*- and *z*-coordinates. This tensor shows coordinate system dependence. The choice of the position for the origins and the orientation for coordinates of all the molecules is the default in the Gaussian03 program.

Accordingly the dipole vectors have been also reduced:

$$\mu_{\text{eff}} = \left(\mu_x^2 + \mu_y^2 + \mu_z^2\right)^{1/2}$$

The stabilization of the *quasi*-planar *trans* conformer of 2-bromostyrene has been rationalized in the framework of the quantum theory Atom-in-Molecules, AIM, using the AIM2000 [37] package. Finally, Natural Bonding Orbital theory has been applied to help to attain at an explanation of the rotation barrier of the selected compounds. To do that, NBO 3.01 [38] code as implemented in Gaussian03 was used.

3. Experimental

Poly-(2-bromostyrene) and poly-(4-bromostyrene) were purchased from Scientific Polymer Products, Inc. USA and used as-received without any further purification. DSC studies were performed on a DSC Q-10 from TA-Instruments. Two heating cycles were performed at heating rate of 20 °C/min, from 0 to 200 °C and the glass transition was determined in the second scan.

4. Results and discussion

4.1. Molecular geometry: 2- bromostyrene

The molecular structure of 2- bromostyrene was determined by Shen et al. in 2001 by electron diffraction [39]. The experimental data are consistent with a non-planar model in which the vinyl group is rotated away from the bromine atom around 152°. They pointed out that only the anti conformer was observed and there was no improvement in the fitting between experimental and theoretical data with the inclusion of the gauche conformer at the temperature of the experiment (378–373 K). They suggested that the absence of the gauche conformer could be due to a Br···H interaction, resulting the *anti* conformer as the sole specie present in the gas phase. *Ab initio* MP2 and DFT methods render a most stable, *quasi*-planar *trans* conformation regardless the basis set wherein the vinyl moiety deviates 22–36° away from the plane defined by the benzene ring. Fig. 1 shows a molecular draw along with the numbering atom.

The predicted torsion angle C4–C3–C1–C8 (see Fig. 1) was 143.7°, 157.5°, 154.5°, 153.4° and 154.2° for MP2/6-31G*, B3LYP/6-31G*, B3LYP/cc-PVTZ and B3LYP/6-311++G** and MPW1PW91/6-31G*, respectively. B3LYP/6-311++G** yields the closest value as compared to the experimental one. The gauche form is 2.3 kcal/mol higher in energy than the *quasi*-planar *trans* form at the B3LYP/6-31G* level, therefore the latter would be the most populated conformation at room temperature (~98%), in agreement with the above-mentioned experimental results.

The experimental and fully optimized geometries of the *quasi*-planar *trans* conformer are listed in Table 1 along with the root-mean-square (rms) deviations between the experimental and calculated sets. As a conclusion, B3LYP/6-31G* hybrid functional yields better results for bond distances and angles than MP2 and mPW1PW91, and hence results are not improved when increasing the size of the basis. B3LYP/6-311++G** yields the best result for the vinyl dihedral angle.

The stabilization of the *quasi*-planar *trans* conformer has been studied by applying the Atoms in Molecules theory [40] to the molecular geometry optimized with B3LYP/6-311++G** (for the B3LYP/6-31G* structure same results are obtained). In this context, the localization of the critical points (CP) is a very suitable tool for the characterization of the molecular electronic structure in terms of the nature and magnitude of the interactions. There are four types of critical points, but only Bond Critical Points (BCPs) and Ring Critical Points (RCPs) will be analyzed in this work. We characterize BCPs and RCPs according to the local properties listed in Table 2: electronic charge density, ρ; Laplacian of the charge density, $\nabla^2\rho$ and the total energy density, *H*. Also of interest for BCP is bond ellipticity, defined as $\epsilon = (\lambda_1/\lambda_2 - 1)$ where λ_1 and λ_2 are the largest and the smallest curvatures of the charge density in a direction perpendicular to the bond path, respectively. The ellipticity provides a measure of the structural stability, that is, substantial bond ellipticities reflect structural instability. Another criterion for structural stability is the distance between a BCP and a RCP. If these two critical points coalesce, they annihilate leading to bond breaking and concomitant ring opening. Fig. 1 shows a schematic picture of the molecule marking all the critical points for both the *quasi*-planar *trans* and the gauche conformations. The small dark spheres are the bond critical points (BCP) and the grey spheres are the ring critical points (RCP).

AIM predicts the existence of a bond path and the corresponding bond critical point BCP (1) between the bromine atom and one hydrogen atom of the vinyl group in the *quasi*-planar *trans* form, and not for the gauche form. *H* and $\nabla^2\rho$ are positive and suggest a Br…H intramolecular contact. Both charge density and Laplacian, with values of 0.0125 a.u. and 0.0469 a.u., respectively, lie within the ranges proposed for these criteria [41], i.e. 0.002–0.035 a.u. and 0.014–0.139 a.u. Ellipticity takes a huge value of 1.906 a.u. and the

Table 1
Experimental and theoretical geometry, root-mean-square (rms) deviations and energies (in Hartrees) calculated for the most stable conformer at different levels of theory for 2-bromostyrene (bond distances are in Å and angles in degrees).

	Exp.[a]	B3LYP/6-31G*	B3LYP/cc-PVTZ	B3LYP/6-311++G**	MP2/6-31G*	MPW1PW91/6-31G*
C1–C3	1.478(11)	1.473	1.469	1.473	1.471	1.468
C3–C4	1.328(21)	1.338	1.331	1.336	1.342	1.335
C1–C2	1.405(3)	1.409	1.404	1.407	1.406	1.404
C2–C5	1.405(3)	1.390	1.384	1.388	1.393	1.387
C5–C6	1.405(3)	1.396	1.390	1.394	1.396	1.392
C6–C7	1.405(3)	1.393	1.387	1.391	1.395	1.389
C7–C8	1.405(3)	1.394	1.388	1.392	1.395	1.390
C8–C1		1.409	1.404	1.407	1.406	1.404
C2–H9	1.109(13)	1.086	1.081	1.083	1.087	1.085
C3–H10	1.109(13)	1.087	1.082	1.085	1.088	1.086
C4–H11	1.109(13)	1.086	1.081	1.083	1.085	1.084
C4–H12	1.109(13)	1.087	1.082	1.085	1.086	1.086
C5–H13	1.109(13)	1.087	1.081	1.084	1.087	1.085
C6–H14	1.109(13)	1.086	1.081	1.084	1.087	1.085
C7–H15	1.109(13)	1.084	1.080	1.082	1.086	1.083
C8–Br16	1.913(6)	1.921	1.920	1.926	1.912	1.899
C1–C3–C4	130.4(37)	125.8	125.7	125.6	123.5	125.4
C2–C1–C3		121.3	121.0	121.0	120.8	121.2
C8–C1–C3	121.8(11)	119.7	122.5	121.0	120.8	122.2
C1–C2–C5		122.1	122.1	122.0	121.7	122.0
C2–C5–C6		119.9	1.390	119.9	119.9	119.9
C5–C6–C7		119.6	119.7	119.7	119.9	119.7
C6–C7–C8		119.6	119.7	119.6	119.3	119.7
C1–C2–C9		118.4	118.4	118.4	118.3	118.4
C1–C3–H10		115.5	115.7	115.8	116.9	115.7
C3–C4–H11		120.8	120.8	120.7	121.1	120.8
C3–C4–H12		122.8	122.6	122.6	121.9	122.6
C2–C5–H13		119.8	119.8	119.8	119.8	119.8
C5–C6–H14		120.7	120.6	120.6	120.5	120.6
C6–C7–H15		120.8	120.6	120.6	120.9	120.9
C7–C8–Br16	117.3(5)	116.9	116.8	116.9	117.7	117.2
C4–C3–C1–C8	152(20)	157.5	154.5	153.4	143.7	154.2
r.m.s.		1.0	1.1	1.1	1.6	1.2
Energy		−2880.7518293	−2883.3831843	−2883.2707628	−2878.016901	−2880.83537541

[a] Ref. [39].

distance between the BCP (1) and RCP (2) is ∼ 0.3 Å. The proximity of those CPs along with the high ellipticity indicate instability of this hydrogen bond [41,42]. Note also that the bond path is curved, pointing out structural instability. Therefore, this interaction may not contribute to a very stable structure leading to a slight change in geometry.

Despite the scarcity of works dealing with RCPs, recently Palusiak and Krygowski [43] have correlated the classical aromaticity indices as HOMA and NICs with AIM parameters showing that the density of total energy, *H*, may serve as a new quantitative characteristic of pi-electron delocalization. The ring critical points of the gauche and *quasi*-planar *trans* conformations have also been analyzed in order to conclude about the higher stabilization of the *quasi*-planar *trans* conformer. To achieve this, electron density, Laplacian, density of the total energy *H*, and its kinetic (*G*) and potential (*V*) components, were analysed at the RCP. Table 2 lists all these parameters. As a result, the ring critical point at the ring center (RCP3 and RCP5) show the same AIM parameters for both gauche and *quasi*-planar *trans* conformer, 4.769 kcal mol^{-1} bohr^{-1}, and also they are very close to the values of *H* for different typical aromatic systems, like for instance benzene and naphthalene, for which these values are in the range 5.128–4.460 kcal mol^{-1} bohr^{-1} [43]. Thus, we could conclude that the different orientation of the vinyl group does not affect the electronic delocalization in the ring. However, the higher value of *H* at the *quasi*-ring RCP2 as compared with RCP4 (see Fig. 1), show a preference for the *quasi*-planar *trans* conformer. Electron density ρ and its Laplacian $\nabla^2\rho$ take also higher values at the RCP2 than at the RCP4, but they are not decisive features to determine the localization/delocalization phenomena within the AIM framework.

Table 2
Local properties of the BCP and RCP in 2-bromostyrene. Values of ρ. $\nabla^2\rho$ and λ_i. are in atomic units. Values of *H*. *G* and *V* are in kcal mol^{-1} bohr^{-1}.

	ρ	$\nabla^2\rho$	λ_1	λ_2	λ_3	*H*	*G*	*V*
BCP1	0.0125	0.0469	−0.0093	−0.0032	0.0594	1.3090	0.0097	−0.0077
RCP2	**0.0124**	**0.0528**	**−0.0088**	**0.0039**	**0.0578**	**1.5060**	**0.0108**	**−0.0084**
RCP3	0.0216	0.1576	−0.0167	0.0830	0.0915	4.7691	0.0319	−0.0243
RCP4	**0.0087**	**0.0408**	**−0.0039**	**0.0096**	**0.0352**	**1.3805**	**0.0079**	**−0.0057**
RCP5	0.0216	0.1579	−0.0168	0.0813	0.0934	4.7691	0.0319	−0.0243

4.2. Molecular geometry: 4-bromostyrene

For 4-bromostyrene, DFT methods predict a planar conformation, except for the MP2 method, which obtains a *quasi*-planar form. The fully optimized geometries and energies are listed in Table 3. To our knowledge, there exists a study of the molecular structure of 4-bromostyrene determined from 1H NMR spectra [44] and the results are consistent with a planar ground-structure. A microwave investigation by Ralowski et al. [45] concluded also that *p*-bromostyrene is planar.

We focused our attention onto the comparison of some geometry parameters between 2- bromo, 4-bromostyrene and the parent system styrene [14,15] in order to determine the influence of the position of the halogen in the structural parameters. The most recent theoretical study of the molecular structure and torsional potential of styrene, performed by Sancho-Garcia and Pérez-Jiménez [15], concluded that *ab initio* (MP2 and Coupled Cluster) methods predict the existence of a global twisted minimum with a slightly lower energy than the planar structure. However, exchange-correlation functionals such as B3LYP are unable to predict this twisted conformation. For bromostyrenes, the same

Table 3
Theoretical geometry and energies calculated for the most stable conformer at different levels of theory for 4-bromostyrene (bond distances are in Å and angles in degrees).

	B3LYP/6-31G*	B3LYP/cc-PVTZ	B3LYP/6-311++G**	MP2/6-31G*	MPW1PW91/6-31G*
C1–C3	1.471	1.468	1.471	1.471	1.467
C3–C4	1.339	1.332	1.336	1.343	1.336
C1–C2	1.407	1.401	1.405	1.405	1.402
C2–C5	1.391	1.385	1.389	1.393	1.387
C5–C6	1.396	1.390	1.394	1.396	1.392
C6–C7	1.392	1.386	1.390	1.395	1.388
C7–C8	1.394	1.389	1.392	1.394	1.390
C8–C1	1.405	1.399	1.403	1.404	1.400
C2–H9	1.086	1.081	1.083	1.087	1.085
C3–H10	1.090	1.085	1.088	1.090	1.089
C4–H11	1.086	1.081	1.083	1.085	1.084
C4–H12	1.087	1.082	1.084	1.086	1.085
C5–H13	1.085	1.080	1.082	1.086	1.083
C6–Br14	1.911	1.911	1.912	1.906	1.892
C7–H15	1.084	1.078	1.082	1.086	1.083
C8–H16	1.087	1.083	1.085	1.089	1.086
C1–C3–C4	127.5	127.6	127.5	125.4	127.4
C2–C1–C3	123.3	123.3	123.3	122.3	123.2
C8–C1–C3	119.0	119.0	119.1	119.5	119.0
C1–C2–C5	121.4	121.4	121.4	121.2	121.3
C2–C5–C6	119.4	119.4	119.4	119.1	119.4
C5–C6–C7	120.9	120.8	120.9	121.2	120.9
C6–C7–C8	119.0	119.0	119.0	118.8	119.0
C1–C2–C9	120.0	120.0	120.1	119.8	120.0
C1–C3–H10	114.4	114.5	114.5	115.9	114.5
C3–C4–H11	120.8	120.8	120.7	121.1	120.8
C3–C4–H12	123.0	122.9	122.9	122.3	123.0
C2–C5–H13	120.6	120.4	120.4	120.7	120.6
C5–C6–Br14	119.5	119.5	119.5	119.4	119.5
C6–C7–H15	120.3	120.4	120.5	120.3	120.2
C7–C8–H16	119.0	119.0	119.0	119.1	119.0
C4–C3–C1–C8	0.0	0.0	0.0	26.1	0.0
Energy	−2880.75321686	−2883.38606030	−2883.2734780000	−2878.015953300	−2880.83610441

behaviour is found in the case of 4-bromostyrene while for 2-bromostyrene DFT and *ab initio* methods predict non-planar minima.

The largest difference for bond distances between 2-bromo and 4-bromostyrene is found for the C–Br bond. This difference amounts to 0.014 Å at the B3LYP/6-311++G** while for the remaining bond distances these differences are within the error limit. For bond angles, C1–C3–C4, C2–C1–C3, C8–C1–C3, C1–C2–C9y C7–C8–Br16 show the largest differences when the position of Br changes from *ortho* to the *para* position, being in the range 2.3°–1.1°. When comparing with styrene [14], the most significant variation in the molecular geometry is found for the C1–C3–C4 bond angle, which takes a similar value for styrene and 4-bromostyrene at the MP2/-31G* and B3LYP/6-31G* levels, while it decreases up to two degrees in the case of 2-bromostyrene.

We have also calculated the rotational barrier of the vinyl–phenyl torsion at the B3LYP level using the 6-31G*, cc-PVTZ and 6-311++G** basis sets together with mPW1PW91 and MP2 levels with the 6-31G* basis set. Figs. 2 and 3 show all the calculated barriers for the different methods essayed in this work.

As can be seen in Figs. 2 and 3, the barrier height from the *cis* conformation is lower in the case of 2-bromostyrene as compared with 4-bromostyrene. However, if we compare the barrier heights from the most stable conformations, which are listed in Table 4, the

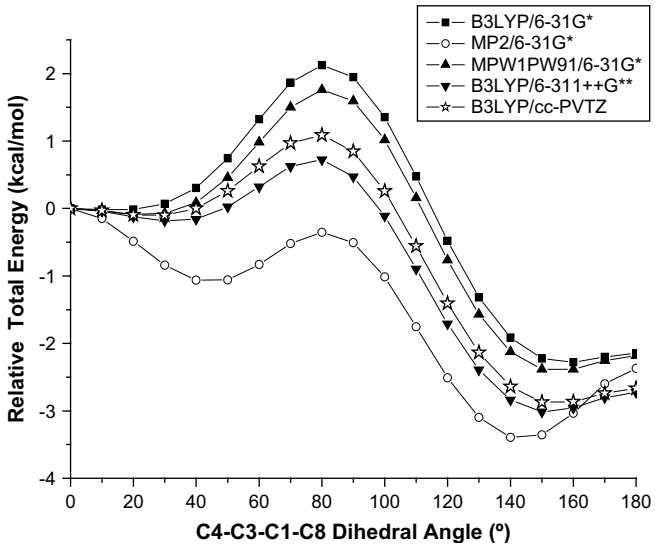

Fig. 2. Torsional potential about the C4–C3–C1–C8 torsion in 2-bromostyrene using different levels of theory.

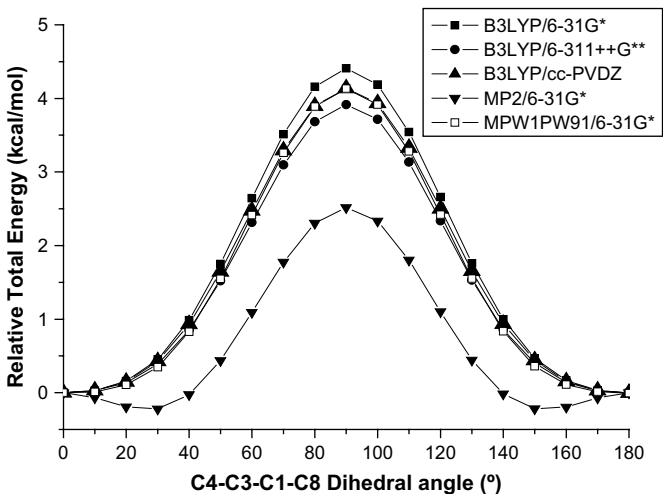

Fig. 3. Torsional potential about the C4–C3–C1–C8 torsion in 4-bromostyrene using different levels of theory.

Table 4
V_i coefficients for the Fourier expansion of the total molecular energy. Barrier height to internal rotation. ΔE(cis–trans) and ΔE (to planarity) in kcal mol^{-1} at different levels of theory for the 2-bromostyrene and 4-bromostyrene at different levels of theory in kcal/mol.

	B3LYP/6-31G*		B3LYP/cc-PVTZ		B3LYP/6-311++G**		MP2/6-31G*		MPW1PW91/6-31G*	
Vi	2Br	4Br	2Br	4Br	2Br	4Br	2Br	4Br	2Br	4Br
V1	−2.631		−3.161		−3.191		−2.803		−2.638	
V2	3.024	4.402	2.191	4.130	1.987	3.904	0.753	2.712	2.691	4.132
V3	0.494		0.473		0.475		0.325		0.447	
V4	−1.011	−0.856	−0.911	−0.802	−0.888	−0.786	−1.341	−0.925	−1.068	−0.905
V5	−0.030		−0.003		0.002		0.048		−0.16	
V6	0.008		−0.003		0.006		−0.063		0.005	
R^2	0.9999	0.9999	0.9998	0.9999	0.9999	0.9999	0.9993	0.9898	0.9999	0.9999
Barrier Height	4.410	4.402	3.985	4.130	3.817	3.904	3.063	2.712	4.153	4.132
ΔE (*cis–trans*)	2.285		2.893		2.926		3.421		2.394	
ΔE (to planarity)	0.1409		0.2259		0.2339		1.0485		0.2138	

values are very similar at each level of theory, showing that the *ortho* or *para* bromine substitution slightly affects the barrier height to vinyl rotation. However, as already studied by the authors [46], when the fluorine atom is at the *ortho* position, the barrier height increases as compared with 2-bromostyrene. Furthermore, the barrier height to planarity for the *quasi*-planar *trans* form amounts to 0.001 and 0.361 kcal/mol for 2-fluorostyrene [46] at the mPW1PW91/6–31G* and MP2/6-31G* levels, respectively, and 0.2138 and 1.0485 kcal/mol for 2-bromostyrene at the same levels of theory. As a result, the *quasi*-planar *trans* conformer is more stabilized than the *cis* one for the bromine substitution than in the case of the fluorine substitution when the halogen is at the *ortho* position. In fact, although the *cis* and *quasi*-planar *trans* conformers are populated enough for 2-fluorostyrene, only the *quasi*-planar *trans* form would be populated for the 2-bromostyrene at room temperature, as already showed from the electron diffraction study [39].

4.3. Internal barrier decomposition schemes

The study of the nature of the barrier to rotation of the vinyl torsion leads us to the foundations of the stabilization of the different conformers. The Total Energy Surface for the target torsion angle was calculated in steps of 10° in the range 0–180° relaxing all the other geometrical parameters. The energy profiles were fitted to a sixth-order Fourier expansion:

$$V(\theta) = \sum_{i=1}^{6} \frac{1}{2} V_{iN}(1 - \cos iN\theta)$$

where N, the symmetry number, is equal to 1 for 2-bromostyrene and 2 for 4-bromostyrene. No contributions to torsional energies from zero-point energy were taken into account.

The decomposition of the total energy function and the analysis of the different terms V_{iN} have previously been shown to be a simple way of analyzing the stabilization of different conformations in molecular systems [47–49]. Table 4 lists the calculated V_{iN} coefficients applying the B3LYP/6-31G*, B3LYP/cc-PVTZ, B3LYP/6-311++G**, MP2/6-31G* and MPW1PW91/6-31G* methods.

The main contributions to the rotational barrier are V_1, V_2, V_3 and V_4. The terms V_{5-6} are less significant in deconvoluting the total energy curve. In the case of 4-bromostyrene, only V_2 and V_4 are present. The relative magnitudes and signs of the main terms are similar regardless the level of theory used except for MP2/6-31G* which predicts V_2 to decrease significantly as compared with the rest of the V_{iN} terms.

Figs. 4 and 5 show the Fourier decomposition of the total energy function from B3LYP/6-31G* for 2- and 4-bromostyrene. As it can be seen, V_2 is barrier forming both for 2-bromostyrene and 4-bromostyrene. Also, from Figs. 4 and 5 one can see that V_1 is large and negative demonstrating that there is a strong preference for a *trans* geometry in the case of 2-bromostyrene. As a result, the substitution of the fluorine atom by bromine in styrene at *ortho* or *para* position leads to a decrease of the V_2 term [46,50].

According to this results for the barriers, and taking into account that B3LYP/6-31G* gives good results for the geometry in the case of 2-bromostyrene, the B3LYP/6-31G* standard method has been selected for further energy decomposition schemes in order to

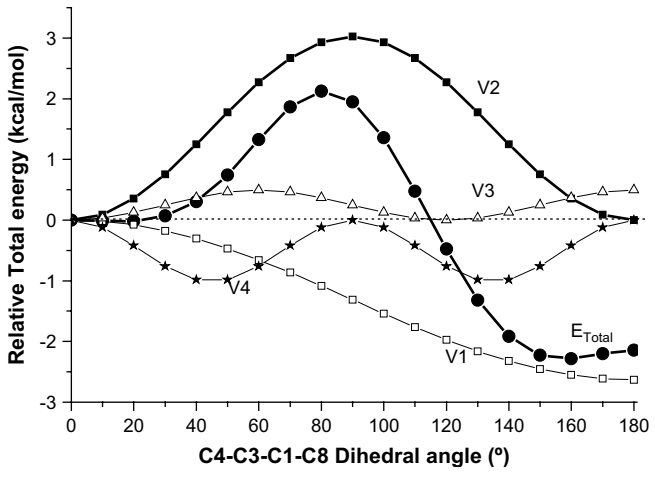

Fig. 4. Fourier decomposition of the potential function $V(\theta)$ for 2-bromostyrene calculated using B3LYP with a 6-31G* basis set.

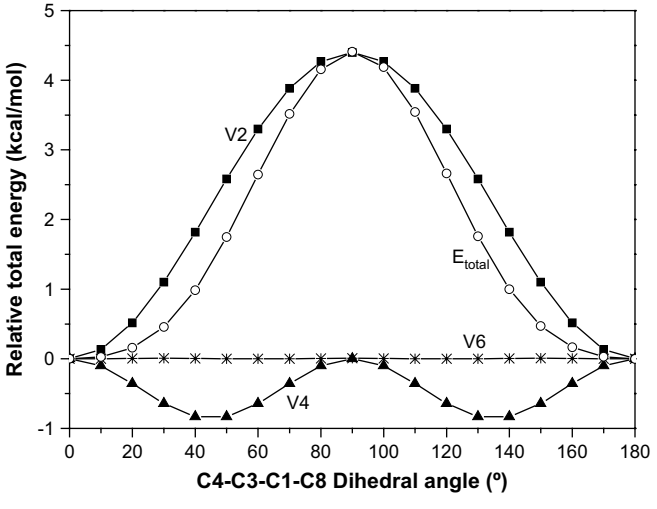

Fig. 5. Fourier decomposition of the potential function $V(\theta)$ for 4-bromostyrene calculated using B3LYP with a 6-31G* basis set.

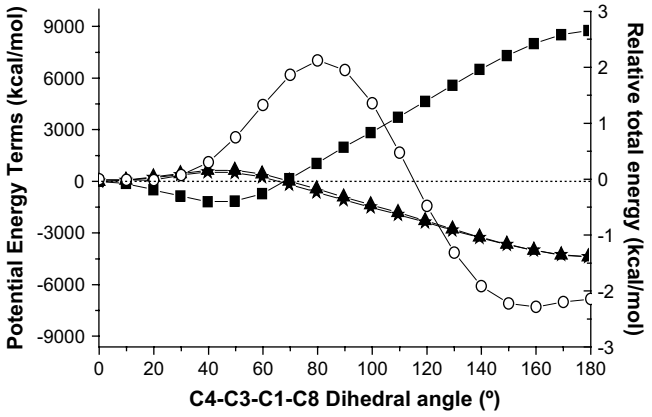

Fig. 6. Dependence of attractive (ΔE_{en} bold squares) and repulsive (ΔE_{nn}, stars, and ΔE_{ee}, bold triangles) energy increments on the C4–C3–C1–C8 rotation angle in 2-bromostyrene at the B3LYP/6–31G* level. The total energy is represented by circles.

investigate the energetic consequences of the vinyl moiety rotation. Thus, the torsion barrier has been characterized using two different schemes. In the first one, the total energy changes are decomposed as a sum of potential and kinetic contributions. In the second one, the natural bond orbital partitioning scheme, NBO, has been applied in order to decompose the total energy in the E_{Lewis} and E_{deloc} terms. According to the first one, we have performed an investigation of the energy barrier based on the partition offered by the scheme:

$$\Delta E = \Delta E_{nn} + \Delta E_{en} + \Delta E_{ee} + \Delta E_{k} \quad (2)$$

where ΔE, ΔE_{nn}, ΔE_{en}, ΔE_{ee} and ΔE_{k} stand for the relative total, nuclear–nuclear repulsion, electron–nuclear attraction, electron–electron repulsion and kinetic energies, respectively, of each conformer with respect to the most stable one. Results after applying this decomposition scheme to the B3LYP/6-31G* energy as a function of the C4–C3–C1–C8 torsion angle are shown in Figs. 6 and 7. For 4-bromostyrene, three different regions can be established: 0°–60°(I), 60°–100°(II) and 100°–180°(III) where the signs of increments ΔE_{ee}, ΔE_{nn} and ΔE_{en} change alternatively. In the I and III regions, the attractive term ΔE_{en} is negative favouring non-planar forms at 40° and 130°, where the repulsive terms takes their largest values. For the central region (II), the repulsive terms favours a perpendicular form (90°). Since the attractive term E_{en} is

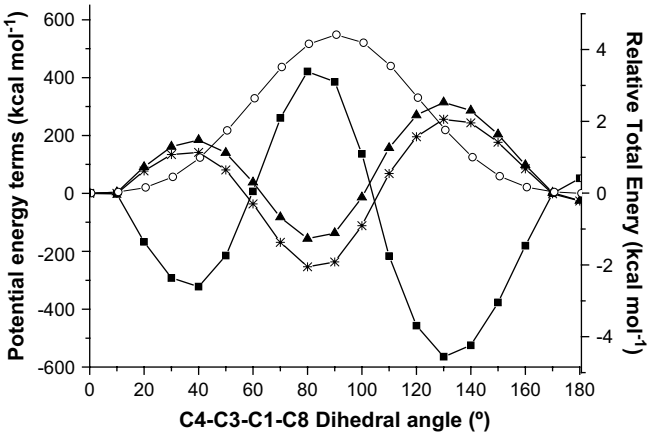

Fig. 7. Dependence of attractive (ΔE_{en} bold squares) and repulsive (ΔE_{nn}, stars, and ΔE_{ee}, bold triangles) energy increments on the C4–C3–C1–C8 rotation angle in 4-bromostyrene at the B3LYP/6-31G* level. The total energy is represented by circles.

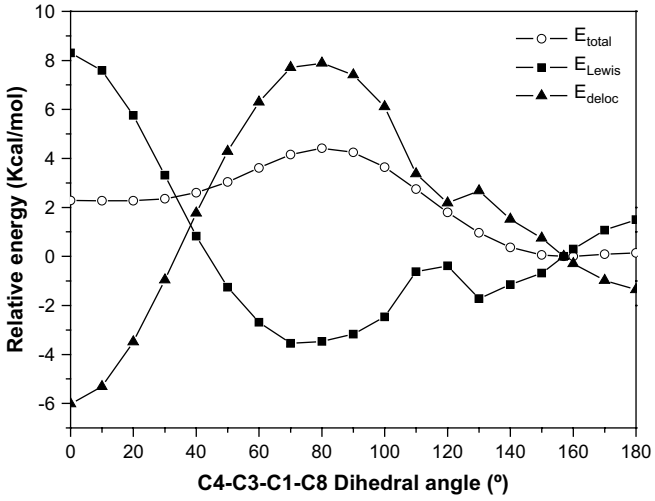

Fig. 8. Dependence of the relative total energy of the 2-bromostyrene molecule and its ΔE_{Lewis} and ΔE_{deloc} parts on the C4–C3–C1–C8 rotation angle at B3LYP/6-31G*.

negative, the highest value of ΔE_{en} at the top of the curve indicates the lowest absolute value of E_{en} at that point.

The real energetic preference in regions I and III which favours the stabilization of the planar form (0° and 180°) is governed by the repulsive terms due to the fact that the sum ($\Delta E_{ee} + \Delta E_{nn}$) is larger than the attractive term, taking its minimum value when going to planarity. In region II, the top of the barrier is governed by the attractive term, which is larger than the sum of both repulsive terms.

For 2-bromostyrene, the repulsive terms favour the *trans* form while the attractive term favours the *cis* one. The sum ($\Delta E_{ee} + \Delta E_{nn}$) is larger than ΔE_{en} at 180° favouring the stabilization of the *trans* form as seen in the total energy curve.

A complementary analysis of the barrier has been performed by analyzing the Lewis and hyperconjugative (non-Lewis) terms according to Eq. (3) on the basis of the natural bond orbital method, NBO [51]:

$$\Delta E_{barrier} = \Delta E_{Lewis} + \Delta E_{deloc} \quad (3)$$

where ΔE_{Lewis} represents the energy of the hypothetical localized species described by a determinant of nearly doubly occupied NBOs

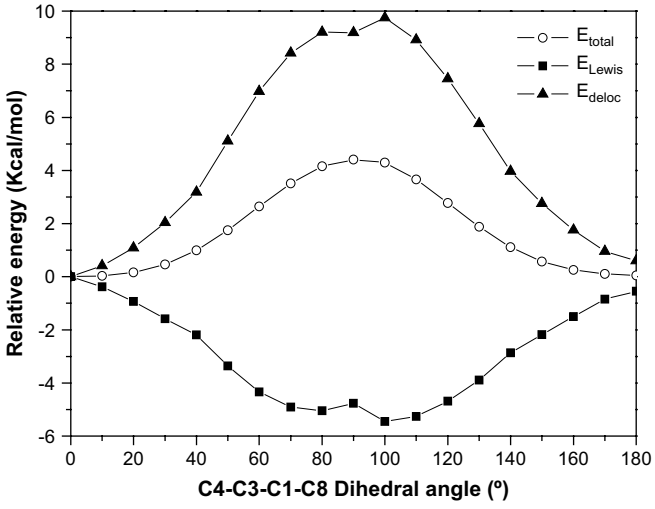

Fig. 9. Dependence of the relative total energy of the 4-bromostyrene molecule and its ΔE_{Lewis} and ΔE_{deloc} parts on the C4–C3–C1–C8 rotation angle at B3LYP/6-31G*.

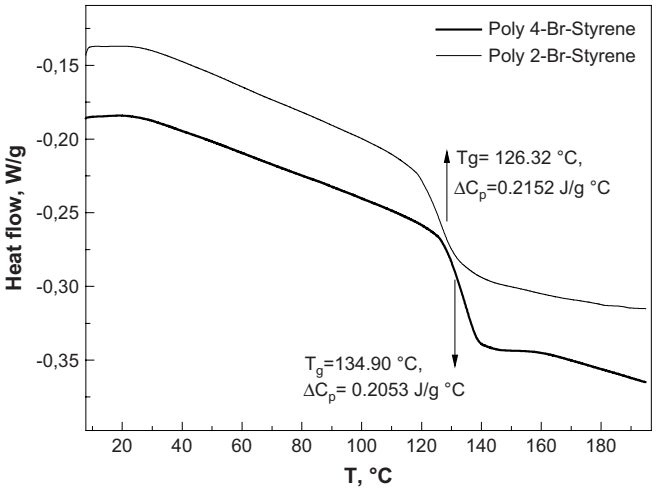

Fig. 10. DSC termograms for poly-2-bromostyrene and poly-4-bromostyrene.

comprising the core, lone-pairs and localized bonds of the Lewis structure and the delocalization energy change, ΔE_{deloc}, represents the hyperconjugative stabilization contribution to the rotational barrier that arises from bond–antibond charge transfer.

The dependence of both components, E_{Lewis} and E_{deloc}, on the vinyl rotation is shown in Figs. 8 and 9 for B3LYP/6-31G*. For both 2-bromostyrene and 4-bromostyrene, hyperconjugation is decisive to explain the energetic preferences since their minima correspond to *cis* and *trans* forms displaying lower energies than the top structure. The minimum of E_{Lewis} carries the information that the top barrier rotamer would have the lowest energy of all rotamers with full occupation of the Lewis bonding orbitals. For 4-bromostyrene, Fig. 9 shows that the delocalization energy E_{deloc} favors a planar conformer whereas the E_{Lewis} favor non-planar forms; therefore E_{deloc} is responsible for the stabilization of the stable planar conformation.

In the case of 2-bromostyrene, Fig. 8 shows how the delocalization energy E_{deloc} favors more the *cis* conformer than the *trans* one. The interplay between the Lewis energy and hyperconjugation is responsible for the stabilization of the *quasi*-planar *trans* form when going to 180° as opposite to the *cis* one.

Once the molecular geometry and torsional barrier for the monomers have been studied, showing that B3LYP/6-31G* is a good choice to predict and explain the stabilization of the different conformations, in the next section of this work we will extend this study to the dimer and tetramer as representative model of the corresponding polymer.

4.4. Dimer and tetramer conformations

As stated at the beginning, the intermolecular forces, free volume and internal rotation barrier play an important role for predicting the glass transition temperature. One question which arises is how sensitive are those quantum mechanical descriptors to small modifications in the molecular structure of the repetitive unit. Such is the case of changing the position of the halogen in the polystyrene system.

In order to approach that issue, in this paper we focus our attention in three molecular parameters related with T_g: the molecular volume, and the dipole and quadrupole moments. In this work, the afore mentioned properties have been analyzed not only for the monomer but also for the dimer and tetramer in order to check their variation with the size of the molecular system. Furthermore, the rotation barrier around the two central dihedral angles in the tetramer has been calculated in order to get some information about the change in C–C chain flexibility when the bromine atom is at the *ortho* or *para* position. We have also obtained the experimental T_g values for both poly-2-bromo and poly-4-bromostyrene. The corresponding termogram is shown in Fig. 10 from which T_g turns out to be 126 °C for poly-2-bromostyrene and 135 °C for poly-4-bromostyrene.

As for the theoretical method, Höfinger et al. [52] performed a study of the method/basis set dependence of the dipole and traceless quadrupole momenta for small molecules. They compared a combination of methods that take into account correlation effects, together with a high-level basis set, that yield molecular momenta close to experimental values. In particular, they essayed *ab initio* and DFT methods in combination with the 6-31G** Pople's and Dunning's basis set. They concluded that DFT functionals such as B3LYP, B3P86 and B3PW91 are very reliable and accurate methods for computing dipole and quadrupole momenta in combination with the aug-cc-PVDZ basis set.

We have chosen again the small 6-31G* basis set along with the hybrid B3LYP functional as a good compromise between the computational resources and the size of the molecular systems, above all in the case of the tetramer. Also, as shown in the previous

Table 5
Energy of the dimers (Hartrees). ΔE with respect the most stable conformer (kcal mol^{-1}). populations (>0.1%). τ_1 and τ_2 dihedral angles.[a] μ_{eff}. θ_{eff} and molecular volume (V) of 2-bromostyrene and 4-bromostyrene at B3LYP/6-31G* level (The data units are Debye for μ_{eff}. Debye Å for θ_{eff} and Å^3 for V).

	Conformer	Energy	ΔE	N_i (%)	τ_1	τ_2	μ_{eff}	θ_{eff}	V
4-bromostyrene	Monomer			100			1.7151	6.3293	174.4
	Dimer1	**−5762.76680418**	**0.00**	**48.5**	**179.3**	**60.9**	**2.3465**	**14.6613**	**363.3**
	Dimer2	**−5762.76630309**	**0.31**	**28.7**	**64.2**	**60.1**	**2.4953**	**12.1608**	**365.1**
	Dimer3	**−5762.76546212**	**0.84**	**11.7**	**−176.3**	**170.9**	**2.4649**	**15.4687**	**367.3**
	Dimer4	−5762.76492679	1.18	6.6	−63.1	170.3	2.4542	15.9588	344.9
	Dimer5	−5762.76435339	1.54	3.6	174.9	−65.5	2.5948	15.6025	372.2
	Dimer6	−5762.76231899	2.81	0.4	76.4	163.1	1.6694	7.8893	365.2
	Dimer7	−5762.76193705	3.05	0.3	−85.9	62.4	3.9710	14.3127	357.4
	Dimer8	−5762.76141990	3.38	0.2	−73.2	−57.7	2.3650	17.6031	368.1
	Dimer9	−5762.75891674	4.95	0	66.9	−79.9	4.0584	15.7762	344.3
2-bromostyrene	Monomer			98			1.6839	5.8849	186.1
	Dimer1	**−5762.7678977**	**0.00**	**31.0**	**178.0**	**58.3**	**1.0213**	**9.2407**	**381.9**
	Dimer2	**−5762.7678355**	**0.04**	**28.9**	**67.5**	**62.2**	**1.6618**	**8.0965**	**364.1**
	Dimer3	**−5762.7678298**	**0.04**	**28.9**	**−173.3**	**168.6**	**2.7139**	**5.5558**	**327.9**
	Dimer4	−5762.7666831	0.76	8.6	178.2	−65.6	1.9449	9.5581	345.7
	Dimer5	−5762.7649310	1.86	1.3	−58.5	169.7	2.3462	4.8383	346.3
	Dimer6	−5762.7642487	2.29	0.6	63.4	143.9	1.5311	7.6236	382.3
	Dimer7	−5762.7638867	2.52	0.4	−88.2	−70.5	1.3900	11.7401	347.6
	Dimer8	−5762.7602317	4.8	0	59.4	−74.6	2.7985	7.9732	364.9

[a] The numbering atom for the dihedral angles τ_1 and τ_2 are defined in Figure 1S as Supporting information.

Table 6
Energy of the tetramers (Hartrees). ΔE with respect the most stable conformer (kcal mol^{-1}). populations (>0.1%). τ_1 and τ_2 dihedral angles.[a] μ_{eff}. θ_{eff} and molecular volume (V) of 2-bromostyrene and 4-bromostyrene at B3LYP/6-31G* level (The data units are Debye for μ_{eff}. Debye Å for θ_{eff} and Å^3 for V).

	Conformer	Energy	*ΔE*	N_i (%)	τ_1	τ_2	μ_{eff}	θ_{eff}	*V*
4-bromostyrene	Tetramer1	−11524.3252242	**0.00**	**48.8**	**177.03**	**−66.03**	**0.6275**	**17.2822**	**723.8**
	Tetramer2	−11524.3252089	**0.01**	**47.9**	**64.01**	**−176.92**	**0.2752**	**18.1087**	**611.1**
	Tetramer3	−11524.3218885	2.10	1.4	138.97	−175.43	2.0520	25.0166	706.0
	Tetramer4	−11524.3209017	2.72	0.5	107.03	−63.09	2.3605	4.1617	715.0
	Tetramer5	−11524.3207334	2.82	0.4	−71.27	−160.99	2.3813	25.7898	752.0
	Tetramer6	−11524.3206356	2.88	0.4	162.74	71.36	2.5835	23.3506	695.3
	Tetramer7	−11524.3205777	2.92	0.3	96.80	74.35	3.2305	28.2943	716.8
	Tetramer8	−11524.3197587	3.43	0.1	−71.96	−91.67	2.6927	12.3514	711.2
	Tetramer9	−11524.3109578	8.92	0	−77.26	48.71	4.0891	15.3107	626.2
2-bromostyrene	Tetramer1	−11524.3322786	**0.00**	**82.8**	**61.3**	**−178.0**	**1.1354**	**3.5845**	**763.1**
	Tetramer2	−11524.3300980	1.36	8.3	−177	−52	2.6452	13.3638	669.8
	Tetramer3	−11524.3300918	1.37	8.2	177.6	65.6	2.2677	9.3159	728.2
	Tetramer4	−11524.3274578	3.02	0.5	163.9	−153.79	3.1192	12.6192	705.2
	Tetramer5	−11524.3265160	3.62	0.2	−65.2	−102.4	1.0656	19.2166	715.7
	Tetramer6	−11524.3248419	4.66	0	149.5	56.9	3.0057	24.5916	688.3

[a] The numbering atom for the dihedral angles τ_1 and τ_2 are defined in Figure 2S as Supporting information.

section, B3LYP/6-31G* is a good method for predicting the geometries of 2-bromostyrene and 4-bromostyrene and has previously been used in QSPR studies yielding good correlations between descriptors and macroscopic properties [4–7].

The most stable conformations for the dimer and tetramer have been optimized at the B3LYP/6-31G* level focusing our attention onto the relative values of the two central dihedral angles (see Fig. 1S and 2S in Supporting information). Because each flexible backbone dihedral angle is expected to have three minima, i.e., +60°, 180°, and −60°, the number of minima that may be anticipated for the potential energy hypersurface is $3^2 = 9$. All the molecular parameters were relaxed during the geometry optimization. The stationary points found for the dimer are listed in Table 5 along with their energy, the relative energy as compared to the preferred conformation, their Boltzman population at 298 K, their dipole and quadrupole momenta and their molecular volumes. Table 6 contains the same information for the tetramer.

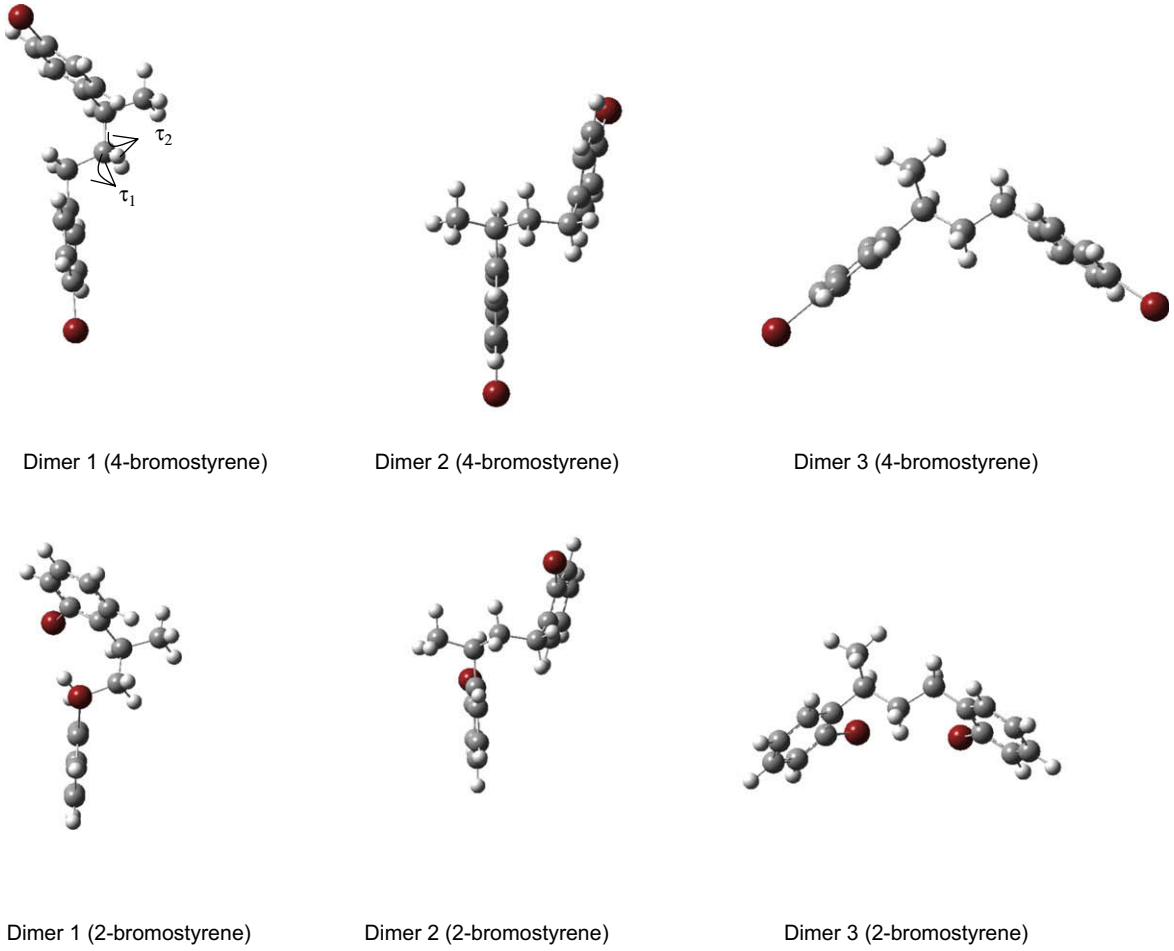

Fig. 11. The most populated dimer conformations for 2-bromostyrene and 4-bromostyrene.

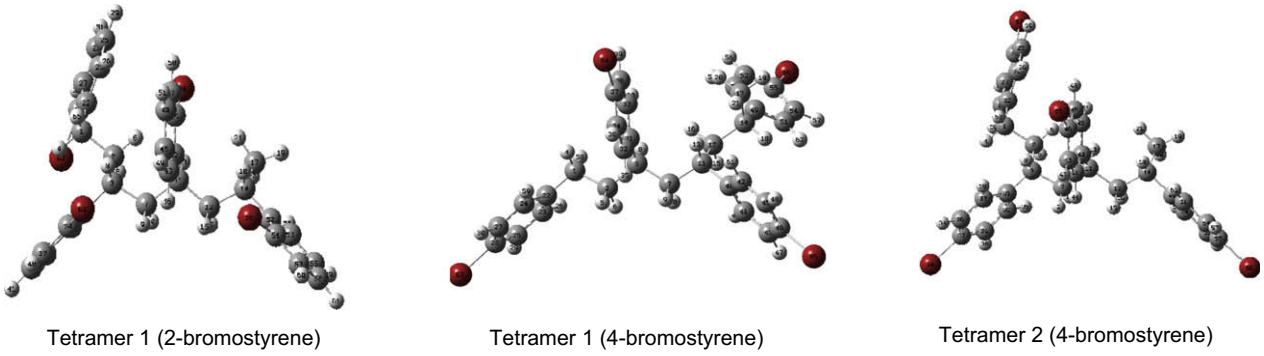

Fig. 12. The most populated tetramer conformations for 2-bromostyrene and 4-bromostyrene.

In the case of the dimer, for both 2- and 4-bromostyrene, the three first conformations amount to over 85% of the population and we will center our discussion on them. These conformers are represented (see Fig. 11). According to the dihedral angles, a *quasi*-T-shaped (Dimer1), a face-to-face (Dimer2) and a mutually perpendicular (Dimer3) structure are stabilized. For both 2- and 4-bromostyrene, the *quasi*-T-shaped structure is predicted to be the most stable although the energy difference with the rest of possible orientations is relatively small.

In the case of the tetramer, two stable conformations are found for 4-bromostyrene and only one populated conformation for 2-bromostyrene (see Fig. 12). If we center our attention on the two central rings, we conclude that they tend to adopt a face-to-face conformation in the case of 2-bromostyrene and in the case of the second conformer of the 4-bromo derivative. For the most stable conformer of 4-bromostyrene, these rings tend to adopt a T-shaped orientation. As a result, the central dihedral angles for the most populated dimer and tetramer of both 2- and 4-bromostyrene take close values pointing out that the position of the halogen do not affect the general arrangement of the backbone.

Finally, the internal rotation barriers around the two central dihedral angles have been computed at the B3LYP/6-31G* level of theory for the most populated tetramers. They are shown in Fig. 13. As can be seen, the barrier heights amount to 6–7 kcal/mol for both 2- and 4-bromostyrene suggesting that the most populated conformations are highly stabilized and rotation around the bonds is not feasible at room temperature in both cases.

4.5. Molecular volume, dipole and quadrupole moments calculations

We have analyzed the molecular volume as a parameter representative of the free space available for rearrangement of the molecule. As only the position of the bromine atom is changed between poly-2-bromostyrene and poly-4-bromostyrene, it could be expected that the *ortho* position would generate more free space due to steric repulsion. DFT calculations at the B3LYP/6-31G* level predict, in the case of the monomer, a larger molecular volume for the 2-bromostyrene than for 4-bromostyrene.

In the case of the dimer, the averaged molecular volume amounts to 365 Å^3 for 4-bromostyrene and it lies in the range 328–382 Å^3 for 2-bromostyrene. Nevertheless, the molecular volume of the most populated tetramer of 2-bromostyrene is the largest, and also larger than any of the two stable oligomers of 4-bromostyrene. Therefore, in spite of the dihedral angles produce similar conformations according to the central dihedral angles, the molecule tends to occupy the largest space when the bromine is at the *ortho* position minimizing the possible steric effect and possibly generating a larger free space for reptation.

As for the dipole and quadrupole momenta of the monomers, they take higher values for 4-bromostyrene than for 2-bromostyrene. Accordingly, poly-4-bromostyrene would be more rigid than poly-2-bromostyrene due to the larger contributions of the electrostatic terms to the intermolecular potential. For the dimer, the trend for the averaged dipole and quadrupole momenta of the most stable conformers is similar to the monomer. The most curious result is found for the quadrupole moments of tetramers. As can be seen in Table 6, the quadrupole moment of the most populated tetramers in 4-bromostyrene increases dramatically while the dipole moment decreases to approach zero. According to this result, quadrupole–quadrupole interactions will play a more important role in the electrostatic terms of the intermolecular potential than dipole interactions for 4-bromostyrene. For 2-bromostyrene, this dramatic change is not observed and the dipole and quadrupole momenta are even smaller than those of the monomer.

As a conclusion, although the internal rotation barriers calculated for the tetramer does not provide conclusive results for the higher chain flexibility in the case of poly-2-bromostyrene, the dipole and quadrupole momenta, as well as the molecular volume calculated for the monomer, dimer and tetramer follow the same trend as the measured T_g for poly-2-bromostyrene and poly-4-bromostyrene demonstrating this way the performance of those descriptors for predicting small variations in glass transition temperatures.

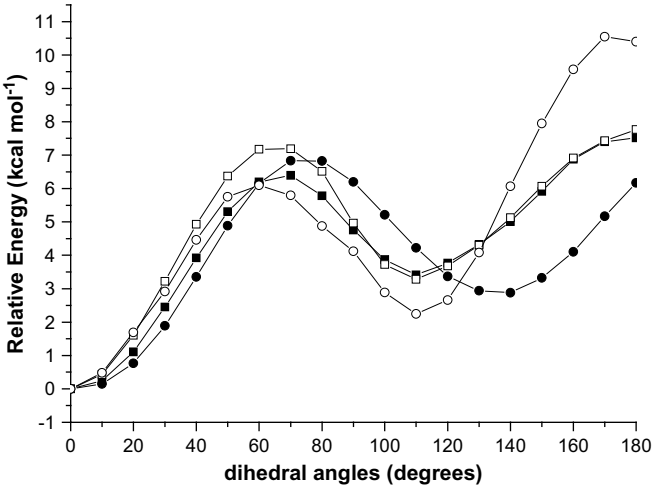

Fig. 13. Torsional potential about the two internal dihedral angles of 4-bromostyrene (circles $\tau_1 = C2–C3–C7–C11$; squares $\tau_2 = C3–C7–C11–C12$) and 2-bromostyrene (bold circles $\tau_1 = C2–C3–C7–C11$; bold squares $\tau_2 = C3–C7–C11–C12$) for the most populated tetramer (Tetramer 1).

5. Conclusions

Quantum chemical descriptors such as dipole and quadrupole momenta, as well as molecular volume, obtained by means of density functional theory have been used to assess the effect of small changes in the molecular structures of the monomer, dimer and tetramer of 2-bromo- and 4-bromostyrene on the glass transition temperature of poly-2-bromo and poly-4-bromostyrene. In addition, correlation with the chain stiffness has been pursued by analysing torsional barriers both for monomer and oligomers of the title compounds obtained at *ab initio* and DFT levels of theory. Internal rotation barrier does not provide conclusive results for the higher chain flexibility in the case of poly-2-bromostyrene, although the dipole and quadrupole momenta as well as the molecular volume follow the same trend as the measured T_g for poly-2-bromostyrene and poly-4-bromostyrene, demonstrating this way the performance of those descriptors in the prediction of small variations in glass transition temperatures. The values of the central dihedral angle for the most populated dimer and tetramer of both 2-bromo and 4-bromostyrene points that the position of the halogen hardly affects the backbone chain arrangement.

Acknowledgements

The authors thank the Spanish Ministerio de Educación y Ciencia (Project MAT 2006-11267) and Junta de Andalucía (PAI-FQM 337 contract and FQM-P06-01864 project) for financial support.

Appendix. Supporting information

Supplementary data associated with this article can be found in the online version, at doi:10.1016/j.polymer.2008.10.041.

References

[1] Sperling LH. Introduction to physical polymer science. 4th ed. New Jersey: Wiley-Interscience; 2006.
[2] Strobl G. The physics of polymers. 3rd ed. Heidelberg, Berlin: Springer-Verlag; 2007.
[3] Mark J, Ngai K, Graessley W, Mandelkern L, Samulski E, Koenig J, et al. Physical properties of polymers. 3rd ed. Cambridge: Cambridge University Press; 2004.
[4] Yu Xinliang, Yi Bing, Wang Xueye, Xie Zhiming. Chem Phys 2007;332:115–8.
[5] Yu Xinliang, Wang Xueye, Li Xiaobing, Gao Jinwei, Wang Hanlu. Macromol Theory Simul 2006;15:94–9.
[6] Liu Tian-Bao, Peny Yan-Fen, Wu Xin-Min. Jiegou Huaxue 2007;26(12):1466–70.
[7] Yu Xinliang, Xie Zhimin, Yi Bing, Wang Xueye, Liu Fang. Eur Polym J 2007; 43:818–23.
[8] Ye Xiangyu, Li Zhen–Hua, Wang Wenning, Fan Kangnian, Xu Wei, Hua Zhongyi. Chem Phys 2004;397:56–61.
[9] Tran Fabien, Weber Jacques, Wesolowski Tomasz A. Helv Chim Acta 2001;84:1489.
[10] Brown Norman MD, Swinton Findlay L. J Chem Soc Chem Commun 1974; 19:770–1.
[11] Hernandez-Trujillo Jesus, Costas Miguel, Vela Alberto. J Chem Soc Faraday Trans 1993;89(14):2441–3.
[12] Meijer EJ, Sprik M. J Chem Phys 1996;105:8684–9.
[13] Baker CM, Grant GH. J Chem Theory Comput 2006;2:947–55.
[14] Choi CH, Kertesz M. J Phys Chem 1997;101A:3823.
[15] Sancho-García JC, Pérez-Jiménez J. J Phys B At Mol Opt Phys 2002;35:1509.
[16] Khare Rajesh, Paulaitis Michael E, Lustig Steven R. Macromolecules 1993;26(26):7203–9.
[17] Ayyagari Chakravarthy, Bedrov Dmitry, Smith Grant D. Macromolecules 2000;33:6194–9.
[18] Adamovic Ivana, Li Hui, Lamm Monica H, Gordon Mark S. J Phys Chem A 2006;110(2):519–25.
[19] Chattopadhyay Sudeshna, Datta Alokmay, Giglia A, Mahne N, Das A, Nannarone S. Macromolecules 2007;40(25):9190–6.
[20] Katada Kinya. Acta Crystallogr 1963;16:290–301.
[21] Meyer Wayne, Bohan Jennifer L, Timberlake Larry D, Siebecker James D. PCT Int Appl 2006:25.
[22] Andersson Patrik L, Oeberg Kjell, Oern Ulrika. Environ Toxicol Chem 2006;25(5):1275–82.
[23] Horie Haruyuki, Shuyama Hideo, Oishi Tsutomu. Polym J 1993;25(7):757–61.
[24] Kosfeld R. Kolloid Zeitschrift 1960;172(2):182–4.
[25] Thaweephan Pawiga, Meng Scott, Sigalov Grigori, Koo Kim Hyun, Sung Choi Ho, Kyu Thein. J Polym Sci Part B Polym Phys 2001;39(14):1605–15.
[26] Frisch MJ, Trucks GW, Schlegel HB, Scuseria GE, Robb M, Cheeseman AJR, Montgomery Jr JA, Vreven T, Kudin KN, Burant JC, Millam JM, Iyengar SS, Tomasi J, Barone V, Mennucci B, Cossi M, Scalmani G, Rega N, Petersson GA, Nakatsuji H, Hada M, Ehara M, Toyota K, Fukuda R, Hasegawa J, Ishida M, Nakajima T, Honda Y, Kitao O, Nakai H, Klene M, Li X, Knox JE, Hratchian HP, Cross JB, Bakken V, Adamo C, Jaramillo J, Gomperts R, Stratmann RE, Yazyev O, Austin AJ, Cammi R, Pomelli C, Ochterski JW, Ayala PY, Morokuma K, Voth GA, Salvador P, Dannenberg JJ, Zakrzewski VG, Dapprich S, Daniels AD, Strain MC, Farkas O, Malick DK, Rabuck AD, Raghavachari K, Foresman JB, Ortiz JV, Cui Q, Baboul AG, Clifford S, Cioslowski J, Stefanov BB, Liu G, Liashenko A, Piskorz P, Komaromi I, Martin RL, Fox DJ, Keith T, Al-Laham MA, Peng CY, Nanayakkara A, Challacombe M, Gill PMW, Johnson B, Chen W, Wong MW, Gonzalez C, Pople JA. Gaussian 03, Revision C.01. Wallingford CT: Gaussian, Inc.; 2004.
[27] Moller C, Plesset MS. Phys Rev A 1934;46:618.
[28] Hehre WJ, Radom L, Scheleyer PVR, Pople JA. Ab initio molecular orbital theory. New York: Wiley; 1986.
[29] Kendall RA, Dunning Jr TH, Harrison RJ. J Chem Phys 1992;96:6796.
[30] Becke AD. J Chem Phys 1993;98:5648.
[31] Lee C, Yang W, Parr RG. Phys Rev A 1988;B37:785.
[32] Perdew JP, Burke K, Ernzerhof M. Phys Rev Lett 1996;77:3865; Erratum. Phys Rev Lett 1997;78:1396.
[33] Adamo C, Barone V. J Chem Phys 1998;108:664.
[34] Wah Wong Ming, Wiberg Kenneth B, Michael J. Frisch Ab initio calculation of molar volumes: Comparison with experiment and use in salvation models. J Comput Chem 1995;16:385.
[35] Buckingham A. Adv Chem Phys 1967;12:107–42.
[36] Eubank PT. AIChEJ 1972;18:454–6.
[37] Biegler-Köning F, Schönbohm J, Bayles D. AIM2000: a program to analyze and visualize atoms in molecules. J Comput Chem 2001;22:545.
[38] Gledening ED, Badenhoop JK, Reed AD, Carpenter JE, Weinhold FF. Theoretical chemistry institute. Madison, WI: University of Wisconsin; 1996.
[39] Shen Q, Kuhns J, Hagen K, Richardson AD. J Mol Struct 2001;567–568:73–83.
[40] Bader RFW. Atoms in molecules: a quantum theory. Oxford: Clarendon Press; 1990.
[41] Popelier PLA. J Phys Chem A 1998;102:1873–8.
[42] Hocquet A. Phys Chem Chem Phys 2001;3:3192–9.
[43] Palusiak M, Krygowski TM. Chem Eur J 2007;13:7996–8006.
[44] Emsley JW, Longeri M. Mol Phys 1981;42(2):315–28.
[45] Ralowski W, Wettermark G, Ljunggren S. Acta Chem Scand 1973;27(5): 1565–72.
[46] Tuttolomondo ME, Navarro A, Peña T, Fernández-Liencres MP, Granadino-Roldán JM, Parker SF, Fernández-Gómez M, sent to publish.
[47] Cramer CJ. Essentials of computational chemistry – theory and models. Wiley; 2004.
[48] Duncan JL. Mol Phys 1974;28:1177.
[49] Bond D, Schleyer PvR. J Org Chem 1990;55:1003.
[50] Granadino-Roldán JM, Fernández-Gómez M, Navarro A, Jayasooriya UA. Phys Chem Chem Phys 2003;5:1760–8.
[51] Reed E, Curtiss LA, Weinhold F. Chem Rev 1988;88(6):899.
[52] Höfinger S, Wendland M. Int J Quantum Chem 2002;86:199–217.